

Performance Evaluation of Ag Doped TiO₂ Nanoflowers in Dye-sensitized Solar Cell

Nurul Najihah Ishak¹, Mohamed Sultan Mohamed Ali^{1*}, Nafarizal Nayan², Megat Muhammad Ikhsan Megat Hasnan², Noor Kamalia Abd Hamed² and Mohd Khairul Ahmad²

¹School of Electrical Engineering, Universiti Teknologi Malaysia, 81310 UTM Johor Bahru, Johor, Malaysia.

²Microelectronics & Nanotechnology-Shamsuddin Research Centre (MiNT-SRC), Institute for Integrated Engineering (I2E), Universiti Tun Hussein Onn Malaysia, 86400 Batu Pahat, Johor, Malaysia.

*Corresponding author: sultan_ali@fke.utm.my

Abstract: Many attempts have been made over the last few years to create effective visible light-activated photovoltaic using Titanium dioxide as photoanode materials in Dye-sensitized solar cell (DSSC). TiO₂ possesses high photocatalytic behavior but has high charge recombination. In this study, the effect of introducing Ag dopant in TiO₂ nanoflower morphology as a blocking layer to reduce charge recombination is investigated. The fabricated Ag doped TiO₂ nanoflower was characterized using XRD, UV-Vis, IPCE, EIS analysis and Solar simulator under 1M solar illumination. Ag dopant may be considered a great approach to improving electron harvesting by suppressing electron recombination between the interface of TiO₂ and electrolyte.

Keywords: DSSC, Hydrothermal method, TiO₂ doped Ag.

© 2021 Penerbit UTM Press. All rights reserved

Article History: received 25 May 2021; accepted 12 June 2021; published 15 September 2021.

1. INTRODUCTION

Dye-sensitized solar cells (DSSCs) are widely regarded as a viable substitute to silicon-based solar cells for photovoltaic (PV) technology in renewable energy harvesting. DSSC was first reported by Gratzel and O'Regan in 1991 recognized with low cost of fabrication, light-weight, lower handling expenses, high mechanical durability, much finer transparency, low toxicity, customizable and flexible design [1], [2]. DSSC is an environmental device as it can generate electricity from light irradiation in electrochemical cells [3]. All components in DSSC contribute significantly to the efficiency, $\eta\%$ of the cell. DSSC comprises of two electrodes which are a working electrode consisting of a photoanode electrode (PE) and anchored dye clamped together with the counter electrode that acts as a catalyst. Redox electrolyte I^-/I_3^- is filled between them and serves as a conductor as shown in Figure 1. PE is an important layer of the DSSC because it creates a surface area for dye adsorption and electron transport. [4], [5].

Titanium dioxide (TiO₂) is the most promising PE material as it exhibits remarkable characteristics of physical and chemical properties [2]. TiO₂ able to withstand photo-corrosion and chemical corrosion and possessed high redox ability. This made TiO₂ a good prospective in a broad range of applications as well as photocatalysis [6], sensor device [7], photoluminescence[8] and solar cell [9]. Photocatalytic activity

of TiO₂ hinged on crystalline form, particle size, and particle shape. Various crystalline formations resulted in different band gaps. For instance, rutile (E_g=3.05 eV), anatase (E_g=3.23 eV), and brookite (E_g=3.26 eV) [10]. Other than that, the morphology of TiO₂ (1-Dimensional, 2-Dimensional and 3-Dimensional) is affected by the anodization state on the photon-to-current efficiency (PCE) of the electrode characteristics. Due to its high large surface area and light scattering, TiO₂ with 3D nanoflower morphology can improve the PCE of DSSC. Yet, the large surface area of TiO₂ can contribute to the dark current due to the aggregation of photoelectrons with oxidized dye and electrolyte [11]. Despite this, the characteristics of TiO₂ are scarce, as spectroscopic studies indicate that approximately 90% of photogenerated electron-hole (e⁻/h⁺) pairs recombine rapidly after the excitation of photon [12]. Thus, this issue led researchers to explore material modification by introducing transition metal ion doping [8], noble metal deposition [12], surface modification [13] and modification by UV illumination to improve the efficiency of DSSC [14].

Reported studies show doping noble metal of silver (Ag) for altering the morphology of TiO₂ nanoparticle structure can reduce charge recombination and increase visible light absorption [15], [16]. In this study, TiO₂ nanoflowers (NFs) doped Ag was fabricated by facile hydrothermal process. The hydrothermal method was employed because crystallization can occur in an aqueous phase at very low temperatures and produces high-purity

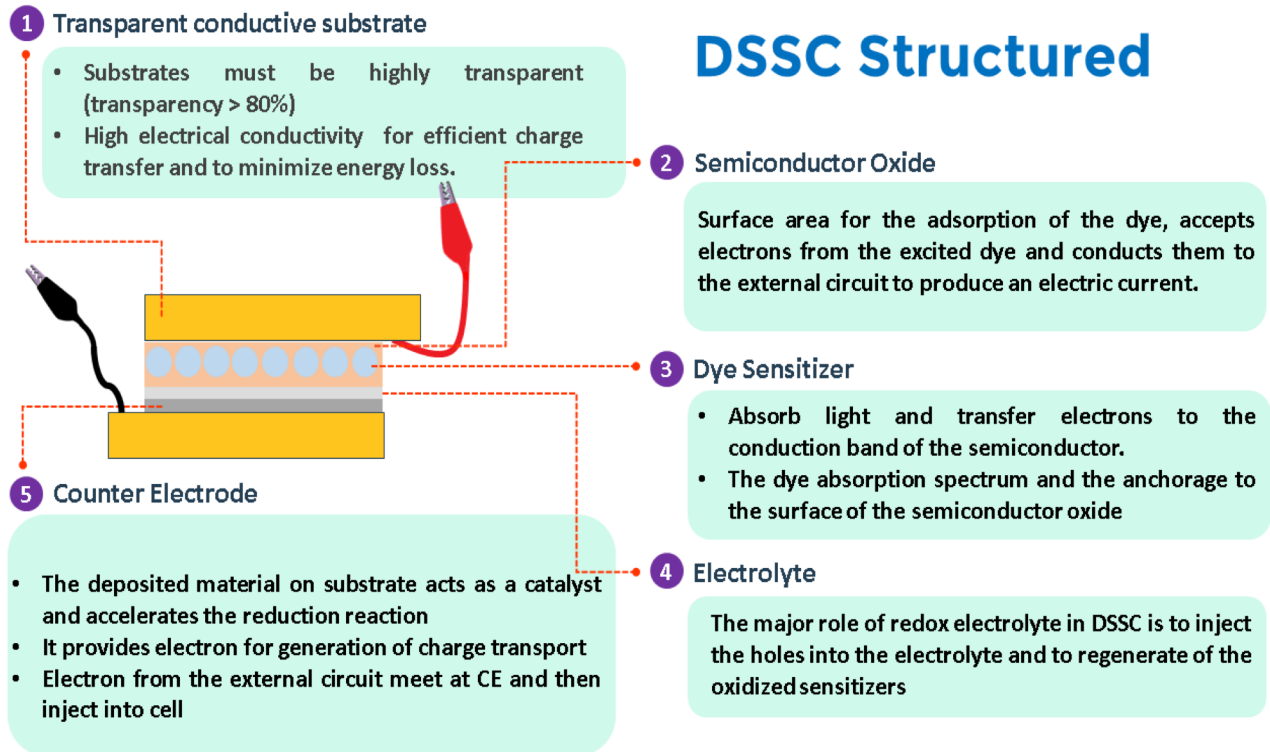


Figure 1. Mechanism of DSSC

crystals with a wide range of forms. The advantages in this work are: (1) three-dimensional TiO₂ NFs can improve the surface area for dye anchoring and light scattering on PE and (2) Ag dopant can exhibit higher visible light absorption and induces Schottky barriers at their interface resulting in lower recombination rate of photo-generated charge carriers. In this study, we investigate PCE of TiO₂ NFs by using varying concentrations of Ag dopant (0.25%, 0.5%, 1.0% and 2.0%) to improve their photovoltaic properties.

2. MATERIALS AND METHOD

TiO₂ doped Ag is synthesized by facile hydrothermal process and deposited on the fluorine-doped oxide (FTO) glass with a dimension of 1.0 (L) × 0.5 (W) × 0.2 (T) cm. The solutions are mixed with 80 ml of deionized water (DI) and 80 ml of hydrochloric acid (HCl) with 36-38% purity in a beaker. Next, the mixed solution is heated at 212 °C for 20 minutes and followed by AgNO₃ (QR&C, USA) solution addition in different weight percentages (0.25%, 0.5%, 1.0%, and 2.0%). The solutions are stirred for 30 minutes while it is heated. The solution is then cooled to room temperature before adding 0.10M Ti(OBu)₄ (No. 5593-70-4, Sigma-Aldrich, Munich, German) dropwise. The mixed solution needs to be stirred until the solution becomes clear [17].

The prepared FTO glass is then arranged in the Teflon-lined autoclave with the sample conducting side facing up. After that, the precursor solution is placed in the autoclave, which is then placed in the oven. This hydrothermal

synthesis takes 10 hours at a constant temperature of 150 °C. Following the synthesis process, the FTO film is removed from the oven and thoroughly rinsed with DI water before being dried in the oven for 30 minutes at 100 °C. There is no post-annealing treatment.

For the preparation of electrolyte, 5 ml of veloronitrile, 10 ml of butyl pyridine (TBP), 10 ml of iodolyte AN 50, 1.597 g DMPII (1.2-dimethyl-3-propylimidazolium iodide) and 0.01g guanidine thiocyanate (GT) are mixed. After mixing the chemicals, the solution is placed in the ultrasonicator for 10 minutes to ensure thorough mixing. The dye solution is then produced using a mixture of 0.0178 g of N719, 25 ml of Acetonitrile, and 25 ml of 1-Butanol. To avoid the solution of dye evaporate, which would cause molarity changes, the solution mixture is then stored at low temperatures (refrigerator's temperature). [18]. The TiO₂ doped Ag films are submerged in the dye for 72 hours (3 days).

Each layer of DSSC is assembling and clamped as shown in Figure 1. The structural characteristics of the photoanode (PE) film at 2θ from 20° to 80° were examined using the X-ray diffraction (XRD) PANalytical X-Pert Powder and HighScore software was used to analyze the data. The optical characteristics and light absorption capabilities of the PE layer are examined using an ultraviolet-visible (UV-vis NIR) spectrophotometer (Shimadzu 3600 Plus spectrophotometer). The efficiency of DSSC is analyzed by using solar simulator (Oriel Sol 1A) with 1 M solar illumination, IPCE and EIS analysis. Table 1 is sample details in this experiment.

Table 1. Sample Details

Samples	Details
A	TiO ₂ Nanoflowers with 0.25% Ag dopant
B	TiO ₂ Nanoflowers with 0.5% Ag dopant
C	TiO ₂ Nanoflowers with 1.0% Ag dopant
D	TiO ₂ Nanoflowers with 2.0% Ag dopant

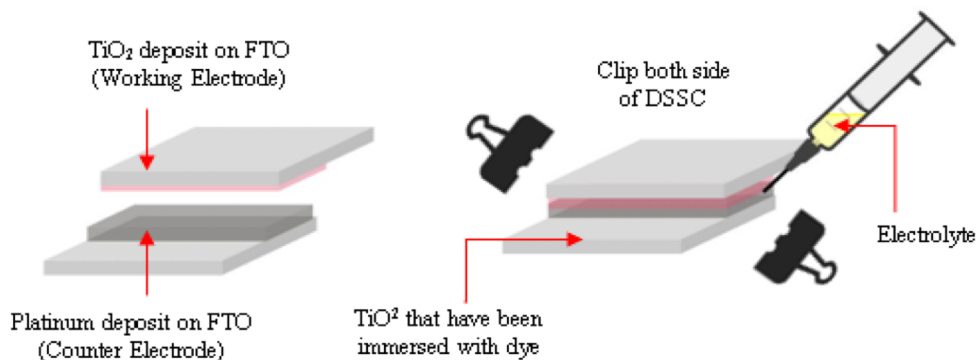


Figure 2. DSSC Assembling

3.0 RESULTS AND DISCUSSION

In this section, the characterization results of XRD, UV-Vis spectrophotometry, Solar Simulator, IPCE and EIS analysis are explained.

3.1 XRD Characterization TiO₂ doped Ag

Figure 3 depicts the crystal structure of TiO₂ doped Ag with different molarities of 0.25%, 0.5%, 1.0%, and 2.0 % estimated in the 20–80° range. There are rutile phase peaks in all of the samples, but no anatase peaks are found. The observed XRD peak corresponded to JCPDS file No. 98-016-8138. The XRD patterns revealed that the pure rutile phase was developed through a simple hydrothermal method that did not involve calcination. Peaks at 2θ of 27.42°, 36.07°, 41.22°, and 54.29° corresponded to the (110), (101), (111), and (211) planes of TiO₂'s rutile form, respectively. According to the studies, XRD peak unable to detect the peak of Ag doped with molarity below 4wt % because of the visibility peak of XRD [17]. Nanoflower TiO₂ in rutile form is good for light-scattering characteristics which are advantageous for DSSC application. Light scattering acts as a photon-trapping system to minimize charge recombination in the DSSC. The light-scattering gives a larger surface area for charge transport of injected electrons within the structure of PE for dye adsorption [4], [19].

3.2 UV-Vis spectral, IPCE and Solar Simulator

The capability of the DSSC to load dye has a significant effect on the incidence of photon-converted electrons (IPCE). In the adsorption of the N719 dye, visible light absorption wavelengths can be detected at 350 nm and 550 nm. Lower current density yields from less dye adsorption which can be validated by UV-Vis spectroscopy. The UV-Vis absorption, bandgap and transmittance spectra of different molarity of 0.25%, 0.5%, 1.0%, and 2.0% Ag dopant of TiO₂ are shown in Figure 4, Figure 5 and Figure 6 respectively. The efficiency of DSSC is dependent on the diffusion of ejected electrons and the capability of the dye sensitizer anchored on the surface of the photoanode layer to absorb light. Thus, optical properties of substrates were observed to investigate the absorption spectra before and after immersed in the N719 dye solution. It can be observed that there is a significantly different absorption intensity between before and after immersed in dye solution in Figure 4. This is due to the degradation of dye. After immersed in the dye solution, the dye molecule is easily exposed to the surroundings and oxidized when there is no sealant attempted on it. Other than that, the light beam of UV-Vis penetrates through the photoanode layer will passing through the ultraviolet (UV) region can reduce the efficiency of dye molecules.

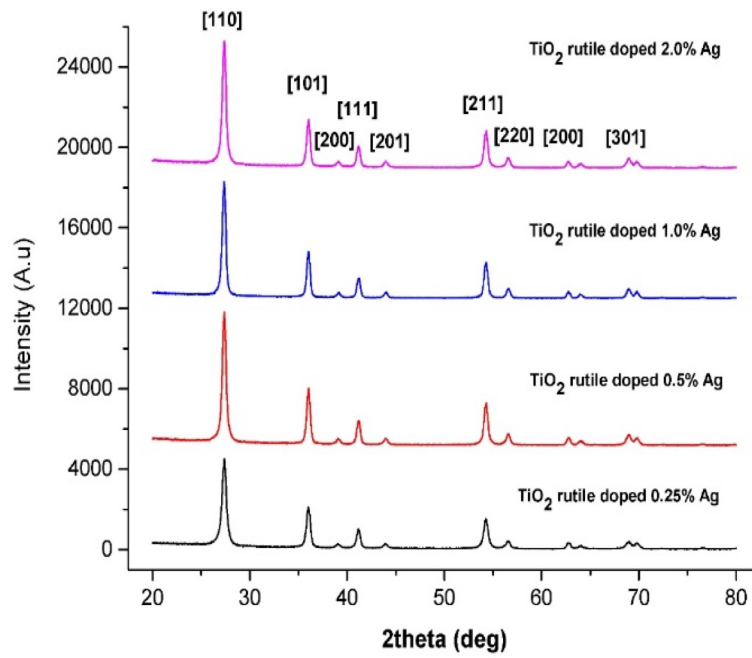


Figure 3. XRD analysis

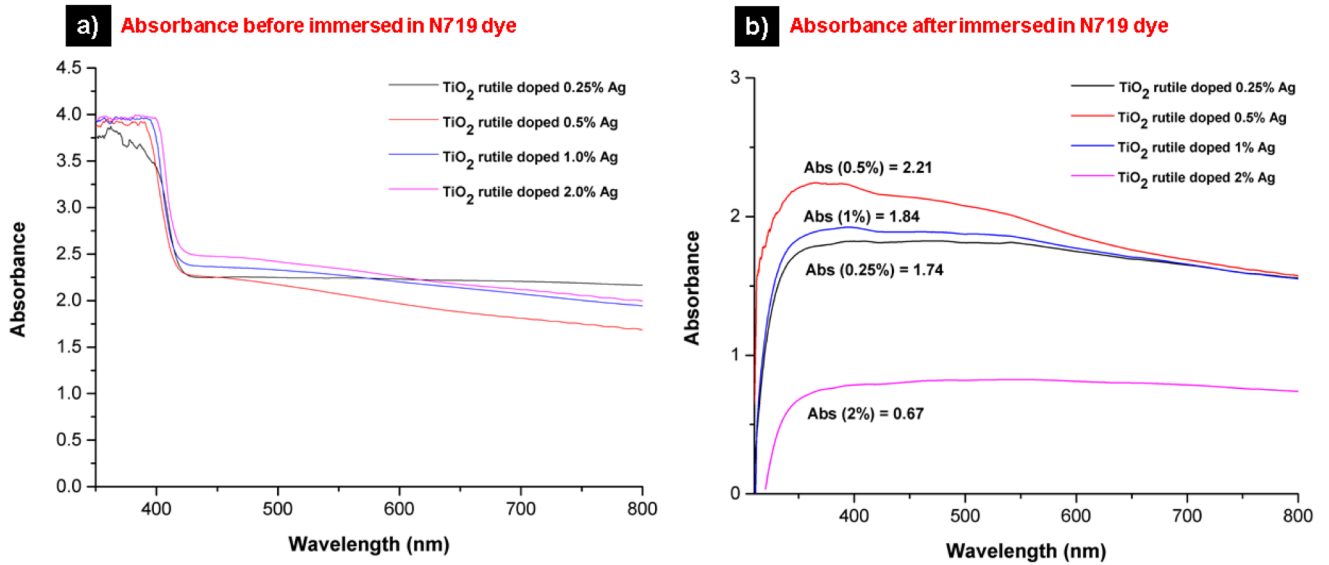


Figure 4. Absorbance before and after immersed in N719 dye

From the absorbance in Figure 4, we can find the bandgap of substrates using the Tauc Plot equation as below [20]:

$$(h\nu\alpha)^{\frac{1}{2}} = A(h\nu - E_g)$$

where $h\nu$ is the photon energy, α is the absorption coefficient, E_g is the absorption bandgap, A is constant [20].

From the Tauc plot equation above, bandgap of TiO_2 doped Ag is 2.89 eV (0.25% doped Ag and 0.5% Ag), 2.90 eV (1% doped Ag) and 2.91 eV (2% doped Ag) as Figure 6. Although TiO_2 is chemically stable in an aqueous solution, the width of the bandgap energy is the significant justification for lower conversion efficiency. Introducing noble metal not only can reduce charge recombination but bandgap energy of TiO_2 as semiconductor photoanode. These are matched with the reported studies [17], [21] that

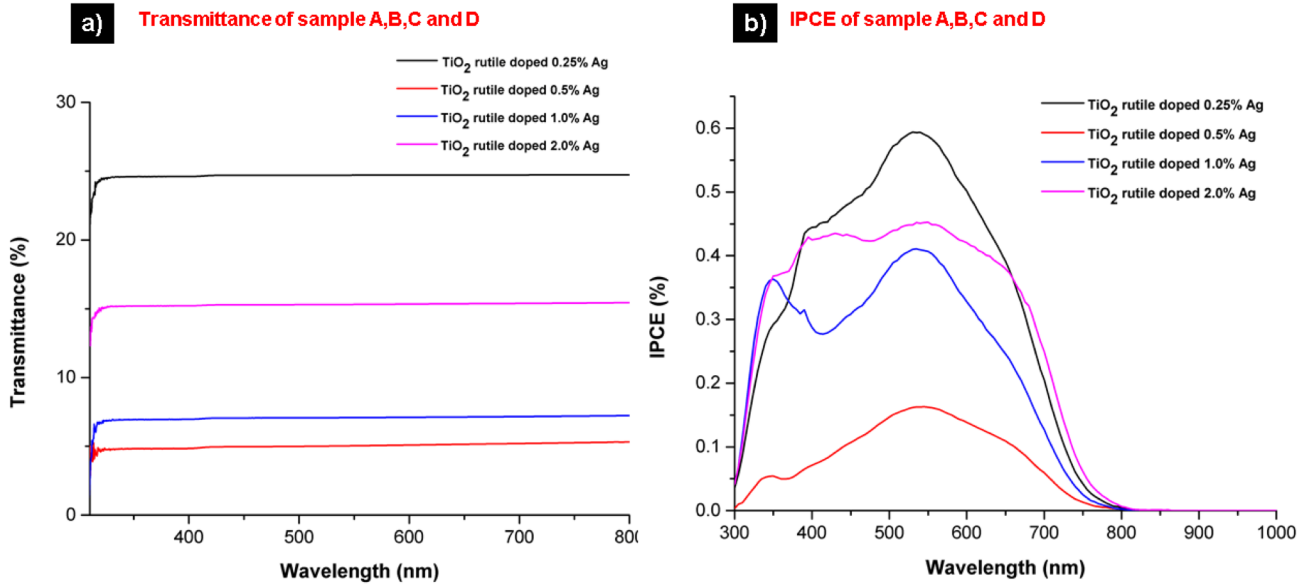


Figure 5. a) Transmittance and b) IPCE of sample A, B, C and D

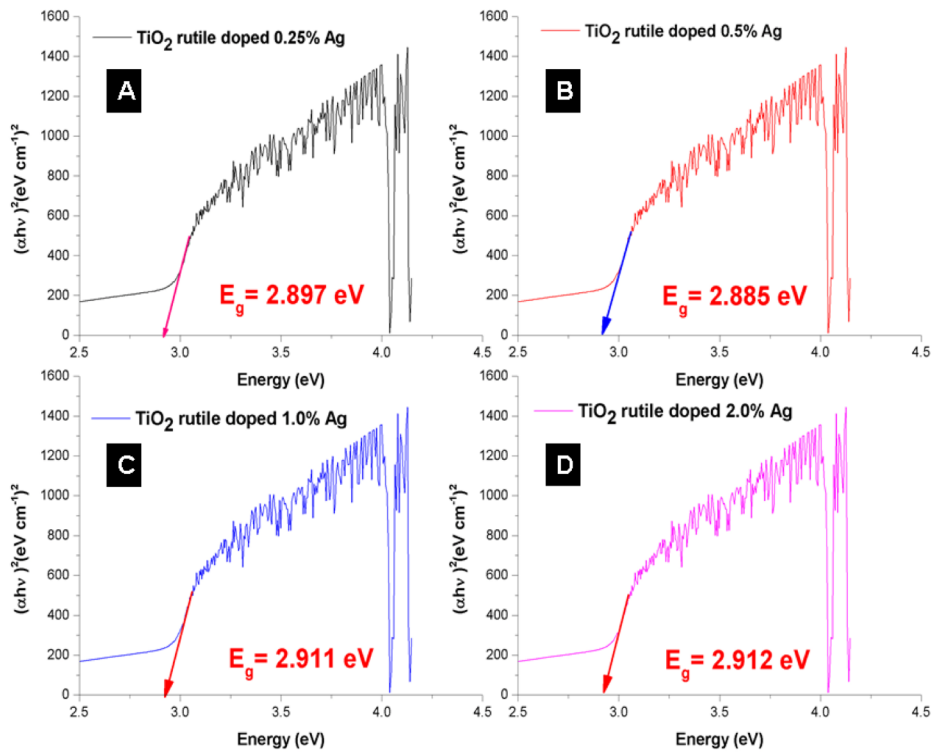


Figure 6. Bandgap sample A, B, C and D

investigate the photocatalytic properties of Ag dopant through bandgap energy.

The lowest bandgap of TiO₂ doped Ag in Figure 6, shows the highest transmittance value as shown in Figure 5 a). Transmittance quantifies the amount of light emitted by the substance and can be expressed mathematically as: [22]:

$$T\% = \frac{1}{Exp(at)}$$

where T, t, and denote the transmittance, thickness, and absorbance coefficients. In Figure 5a), TiO₂ doped with 0.25% Ag demonstrated the highest transmittance spectra. The value transmittance of a substance reflects on how much light irradiation passed through it.

According to Figure 5b), the smallest dopant concentration of 0.25% Ag doped has the highest IPCE, which is the ratio of the number of carriers captured by the solar cell to the number of photons with given incident energy on the solar cell. Next, Table 2 shows the photon-conversion efficiency (PCE) with the highest value using Solar Simulator. The highest 0.25% Ag doped transmittance results are matched with the result of IPCE and PCE. From the results obtained, we can analyze that the thickness of substrates in increasing dopant concentration can affect the optical transmittance, PCE and IPCE materials. Besides, the resistivity of FTO glass also contributes to low transmittance. In this experiment, the resistivity of FTO is measured to be 7 Ω/sq.

Table 2. PCE TiO₂ doped Ag

Sample	V _{oc} , (A)	I _{sc} , (A)	J _{sc} , (mA/cm ²)	Fill Factor	η %
A	0.669	0.0016	3.23	58.08	1.25
B	0.668	0.0013	2.70	53.36	0.96
C	0.653	0.0009	1.79	65.45	0.76
D	0.677	0.0064	2.84	32.88	0.63

3.3 EIS analysis

EIS (electrochemical impedance spectroscopy) is a reliable measure that is being used to investigate electronic and ionic mechanisms in DSSC. The resistance of the interface between electrolyte and counter electrode is represented by the first semicircle in EIS at high frequency (R₁). The resistance of the interface between the electrolyte and the TiO₂ layer is described by a second semicircle at an intermediate frequency (R₂). The third semicircle is looking into the peak frequency associated with electron transport and the back reaction of the photoanode-electrolyte interface (R₃). Table 3 represents the obtained parameters from fitting the EIS plots whereas R_{ct} is the charge transfer resistance of the charge recombination process at the TiO₂/I₃⁻ in the electrolyte which is the value of the impedance in its real component; R_{pt} is the charge transfer resistance Platinum at the counter electrode, R_d is the diffusion resistance and R_s is the resistance of solution. Figure 7 depicts the Nyquist plots from EIS analysis of various samples A, B, C, and D under light illumination.

To correlate with the highest efficiency in this experiment which is sample A (1.25%), the R_{CT} result of sample A showed the third lowest (208.5 Ω) but obtained the lowest R_d (52.55 Ω). This is a significant reason for the current density of sample A which is the highest compared to others (3.23 mA/cm²). Compared the sample D which obtained the lowest efficiency (0.63%), the sample showed the lowest R_{CT} (89.13 Ω) but 1 magnitude higher than R_d sample A (118.4 Ω). This may due to the charge trapping effect of Ag doped and corresponded from the highest bandgap of Sample D from Tauc Plot equation.

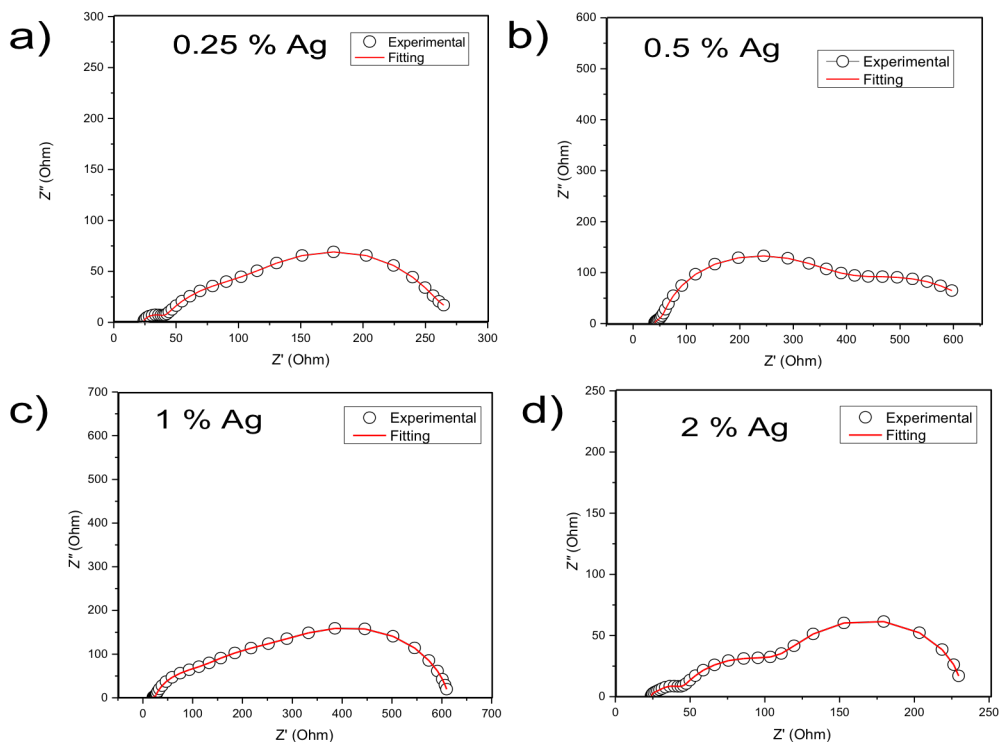


Figure 7. Nyquist plot from EIS analysis under illumination

Table 3. Parameter values of R_s , R_{pt} , R_{ct} and R_d of DSSC photoanode obtained from fitting method

Sample	R_s (Ω)	R_{pt} (Ω)	R_{ct} (Ω)	R_d (Ω)
A	23.11	16.55	208.54	52.55
B	39.8	11.88	312.83	309.1
C	19.58	5.21	251.07	339
D	23.8	4.589	89.13	114.8

4. CONCLUSION

This study shows how a hydrothermal reaction can be used to boost the morphology of TiO_2 nanoflowers doped with Ag. The addition of Ag-doping increased their surface area and visible light absorption. Among the samples, TiO_2 doped 0.25 % wt. Ag had the highest performance, $\eta\%$ (1.25 %). Metal doping has an effect on the band structure and trap states on the surface of TiO_2 . The charge injection between photoanode and dye molecule should be fast to avoid recombination. As a result, a suitable band level is needed to minimize charge recombination. For efficient electron injection, the photoanode and material band edges should match the dye's bandgap structure. To summarize, the bandgap of TiO_2 should be less than 3.0 eV to improve photocatalytic activity in DSSC applications. This is due to the lower bandgap's ability to expand TiO_2 's spectral response to the visible spectrum, as the DSSC mechanism works well in the visible region but degrades in the UV region.

ACKNOWLEDGMENT

We would like to express our gratitude for the financial support provided by the Fundamental Research Grant Scheme (FRGS) Vot K256 and the Microelectronics and Nanotechnology-Shamsuddin Research Centre (MiNT-SRC) for the characterization equipment. Mohamed Sultan thank the Universiti Teknologi Malaysia for Industry-International Incentive Grant (IIIG Q.J130000.3651.03M03) and Altec Industrial & Engineering Supply Sdn Bhd for Contract Research Grant (R.J130000.7651.4C371).

REFERENCES

- [1] N. Kaur *et al.*, "Ag ion implanted TiO_2 photoanodes for fabrication of highly efficient and economical plasmonic dye sensitized solar cells," *Chem. Phys. Lett.*, vol. 740, no. December 2019, 2020.
- [2] Y. X. Dong, X. L. Wang, E. M. Jin, S. M. Jeong, B. Jin, and S. H. Lee, "One-step hydrothermal synthesis of Ag decorated TiO_2 nanoparticles for dye-sensitized solar cell application," *Renew. Energy*, vol. 135, pp. 1207–1212, 2019.
- [3] K. Sharma, V. Sharma, and S. S. Sharma, "Dye-Sensitized Solar Cells: Fundamentals and Current Status," *Nanoscale Res. Lett.*, vol. 13, 2018.
- [4] N. A. Karim, U. Mehmood, H. F. Zahid, and T. Asif, "Nanostructured photoanode and counter electrode materials for efficient Dye-Sensitized Solar Cells (DSSCs)," *Sol. Energy*, vol. 185, no. January, pp. 165–188, 2019.
- [5] Y. Wang *et al.*, "Thickness effect of nanocrystal TiO_2 photoanodes on Dye Sensitized Solar Cells (DSSC) performances," *ICSICT 2012 - 2012 IEEE 11th Int. Conf. Solid-State Integr. Circuit Technol. Proc.*, pp. 10–12, 2012.
- [6] A. R. M. Dalod, L. Henriksen, T. Grande, and M. A. Einarsrud, "Functionalized TiO_2 nanoparticles by single-step hydrothermal synthesis: The role of the silane coupling agents," *Beilstein J. Nanotechnol.*, vol. 8, no. 1, pp. 304–312, 2017.
- [7] A. Di Paola, M. Bellardita, and L. Palmisano, *Brookite, the least known TiO_2 photocatalyst*, vol. 3, no. 1. 2013.
- [8] J. Y. Do, J. Kim, Y. Jang, Y. K. Baek, and M. Kang, "Change of band-gap position of MTiO_2 particle doped with 3d-transition metal and control of product selectivity on carbon dioxide photoreduction," *Korean J. Chem. Eng.*, vol. 35, no. 4, pp. 1009–1018, 2018.
- [9] Y. H. Nien *et al.*, "Enhanced photovoltaic conversion efficiency in dye-sensitized solar cells based on photoanode consisting of $\text{TiO}_2/\text{GO}/\text{Ag}$ nanofibers," *Vacuum*, vol. 167, no. December 2018, pp. 47–53, 2019.
- [10] S. C. T. Lau, J. Dayou, C. S. Sipaut, and R. F. Mansa, "Development in photoanode materials for high efficiency dye sensitized solar cells," *Int. J. Renew. Energy Res.*, vol. 4, no. 3, pp. 665–674, 2014.
- [11] S. Xuhui, C. Xinglan, T. Wanquan, W. Dong, and L. Kefei, "Performance comparison of dye-sensitized solar cells by using different metal oxide-coated TiO_2 as the photoanode," *AIP Adv.*, vol. 4, no. 3, pp. 0–7, 2014.
- [12] A. K. Gupta, P. Srivastava, and L. Bahadur, "Improved performance of Ag-doped TiO_2 synthesized by modified sol-gel method as photoanode of dye-sensitized solar cell," *Appl. Phys. A Mater. Sci. Process.*, vol. 122, no. 8, 2016.
- [13] Y. Kim, C.-H. Yoon, K.-J. Kim, and Y. Lee, "Surface modification of porous nanocrystalline TiO_2 films for dye-sensitized solar cell application by various gas plasmas," *J. Vac. Sci. Technol. A Vacuum, Surfaces, Film.*, vol. 25, no. 4, pp. 1219–1225, 2007.

- [14] L. Li, R. Chen, G. Jing, G. Zhang, F. Wu, and S. Chen, "Improved performance of TiO₂ electrodes coated with NiO by magnetron sputtering for dye-sensitized solar cells," *Appl. Surf. Sci.*, vol. 256, no. 14, pp. 4533–4537, 2010.
- [15] Y.-H. Nien *et al.*, "Study of How Photoelectrodes Modified by TiO₂ / Ag Nanofibers in Various Structures Enhance the Low Illumination," *Energies*, vol. 13, 2020.
- [16] R. Dagherir, P. Drogui, and D. Robert, "Modified TiO₂ for environmental photocatalytic applications: A review," *Ind. Eng. Chem. Res.*, vol. 52, no. 10, pp. 3581–3599, 2013.
- [17] N. K. A. Hamed *et al.*, "Dependence of photocatalysis on electron trapping in Ag-doped flowerlike rutile-phase TiO₂ film by facile hydrothermal method," *Appl. Surf. Sci.*, vol. 534, no. August, p. 147571, 2020.
- [18] F. I. M. Fazli *et al.*, "Rutile-phased Titanium Dioxide (TiO₂) Microstructures by Hydrothermal Method for Dye-Sensitized Solar Cell (DSSC)," *Int. J. Eng. Technol.*, vol. 8, pp. 62–67, 2019.
- [19] S. Ito *et al.*, "Fabrication of thin film dye sensitized solar cells with solar to electric power conversion efficiency over 10%," *Thin Solid Films*, vol. 516, no. 14, pp. 4613–4619, 2008.
- [20] N. Ahmad, F. Mohamad, M. K. Ahmad, and A. Talib, "Influence of growth temperature on TiO₂ nanostructures by hydrothermal synthesis," *Int. J. Eng. Adv. Technol.*, vol. 8, no. 6 Special Issue 3, pp. 936–941, 2019.
- [21] S. K. Md Saad *et al.*, "Two-Dimensional, Hierarchical Ag-Doped TiO₂ Nanocatalysts: Effect of the Metal Oxidation State on the Photocatalytic Properties," *ACS Omega*, vol. 3, no. 3, pp. 2579–2587, 2018.
- [22] M. I. Khan *et al.*, "Effect of silver (Ag) ions irradiation on the structural, optical and photovoltaic properties of Mn doped TiO₂ thin films based dye sensitized solar cells," *Ceram. Int.*, vol. 47, no. October 2020, pp. 15801–15806, 2021.